



Radar Target Scattering Signature for Earth Observation

Abhinav Verma^{*(1)}, Subhadip Dey⁽²⁾, Carlos López-Martínez⁽³⁾⁽⁴⁾, and Avik Bhattacharya⁽¹⁾
 (1) Microwave Remote Sensing Lab (MRSLab), Indian Institute of Technology Bombay, India
 (2) Microwaves and Radar Institute, German Aerospace Centre (DLR), Germany
 (3) Universitat Politècnica de Catalunya (UPC), Barcelona, Spain
 (4) Institute of Space Studies of Catalonia (IEEC), Barcelona, Spain

Abstract

This work extends the polarimetric signature (PS) concept from full polarimetric Synthetic Aperture Radar (SAR) data to compact polarimetric SAR data, following the wide application of this mode for land cover characterization. We first demonstrate the variation of PS for several elementary targets and then illustrate its utility for improved characterization of various natural & human-made targets. We found that the compact-pol signature (CPS) allows enhanced discrimination among the land cover targets, viz., waterbody, different types of the urban area, and vegetation. The proposed method holds significant interest for the Radar Constellation Mission (RCM) datasets and future compact polarimetric SAR missions for enhanced target characterization.

1 Introduction

With the availability of the polarimetric Synthetic Aperture Radar (SAR) datasets for Earth observation, new techniques are needed for optimal utilization of these datasets for land cover applications. The polarimetric signature (PS) is one technique that can enhance the characterization of diverse land cover targets.

In general, the polarimetric SAR (PolSAR) data are expressed in terms of a scattering matrix \mathbf{S} [1]. The \mathbf{S} represents the scattering coefficient measured with a specific polarization basis, usually in the linear transmit-received antenna basis (H-V). However, the \mathbf{S} measured in a particular polarization basis might not provide optimum scattering response from targets possessing complex geometry. Hence, one can synthesize the received power for any combination of transmit-receive antenna polarization basis using the technique known as polarization synthesis [2].

The synthesized received power at all ellipticity ($-45^\circ \leq \chi \leq 45^\circ$) and orientation angle ($-90^\circ \leq \psi \leq 90^\circ$) is known as polarization signature (PS). The ellipticity (χ) and orientation (ψ) angle describes the polarization of the transmit and receive antenna. The concept of PS for a full-polarimetric (FP) SAR data was introduced by van Zyl et al. [3].

The PS technique has been utilized to differentiate point targets and distributed targets [4], and diverse applications viz. land cover feature identification & extraction, crop monitoring [5], and human-made target identification & characterization [6]. Recently, Verma et al., [6] proposed the PS for dual-polarimetric (DP) SAR data and found it useful for enhanced characterization of human-made targets.

Considering the usefulness of PS for land cover target characterization and the availability of the compact-polarimetric (CP) mode SAR data in the recent Earth observation missions, we extend the concept of PS to CP SAR data in the study. The study presents the analysis and comparison of the CP and FP SAR signatures of several elementary, natural & human-made targets.

2 Methodology

We utilize the FP C-band RADARSAT-2 data acquired over San Francisco Bay area to generate the full- and compact-pol SAR signature. The data is calibrated and multilooked to form the coherency matrix \mathbf{T} . Next, we apply a 3×3 refined lee speckle filter to reduce the existing speckle in the image. It is finally terrain corrected to get the geo-location of each pixel.

Further, the \mathbf{T} of FP is converted to the 4×4 real-valued Kennaugh matrix \mathbf{K} to generate the full-polarimetric signature (FPS). Finally, the \mathbf{K} , along with the Stokes vector that describes the polarization basis of the transmitting and receiving antenna, is used to calculate the received power (P). The FPS is then generated by synthesizing the received power, $P(\chi_r, \psi_r, \chi_t, \psi_t)$, for all possible polarization basis of the transmitting and receiving antenna by varying the ellipticity (χ) and orientation (ψ) angle of the transmit (χ_t, ψ_t) and receive (χ_r, ψ_r) antenna [3].

$$P_{FP}(\psi_t, \chi_t, \psi_r, \chi_r) = \begin{bmatrix} 1 \\ \cos 2\chi_r \cos 2\psi_r \\ \cos 2\chi_r \sin 2\psi_r \\ \sin 2\chi_r \end{bmatrix}^T \mathbf{K} \begin{bmatrix} 1 \\ \cos 2\chi_t \cos 2\psi_t \\ \cos 2\chi_t \sin 2\psi_t \\ \sin 2\chi_t \end{bmatrix} \quad (1)$$

where $\chi_t, \psi_t, \chi_r,$ and ψ_r are the ellipticity and orientation angle of the receive and transmit antenna polarization, respectively. The superscript T denotes vector transpose.

In this study, we extend the concept of polarimetric signature for FP SAR data [3] to compact-pol SAR data. We extracted the compact-pol (CP) SAR data in LHV (left circular transmit and linear horizontal and vertical receive) and RHV (right circular transmit and linear horizontal and vertical receive) mode from the FP RADARSAT-2 data mentioned earlier.

On a single-pixel single-look complex level, the CP SAR system measure a projection of the complex scattering matrix \mathbf{S} . Then, the single-look complex data is multilooked to form the 2×2 Hermitian positive semi-definite wave covariance matrix \mathbf{J} . It contains the complete parametric information for a particular circular transmit channel C (L for left circular and R for right circular) and simultaneous linear horizontal (H) and vertical (V) receive.

$$\mathbf{J} = \begin{bmatrix} \langle E_{\text{HC}} E_{\text{HC}}^* \rangle & \langle E_{\text{HC}} E_{\text{VC}}^* \rangle \\ \langle E_{\text{VC}} E_{\text{HC}}^* \rangle & \langle E_{\text{VC}} E_{\text{VC}}^* \rangle \end{bmatrix} \quad (2)$$

where $\langle \dots \rangle$ represents the ensemble average of the covariance matrix elements, and $*$ represents the complex conjugate. Using \mathbf{J} , the four components of the Stokes vector ($\tilde{\mathbf{S}}$) of the scattered wave $\tilde{\mathbf{S}}_s$ can be computed as

$$\mathbf{g}_s = \begin{bmatrix} \langle g_0 \rangle \\ \langle g_1 \rangle \\ \langle g_2 \rangle \\ \langle g_3 \rangle \end{bmatrix} = \begin{bmatrix} \langle |E_{\text{LL}}|^2 \rangle + \langle |E_{\text{LL}\perp}|^2 \rangle \\ \langle |E_{\text{LL}}|^2 \rangle - \langle |E_{\text{LL}\perp}|^2 \rangle \\ 2\Re \langle E_{\text{LL}} E_{\text{LL}\perp}^* \rangle \\ 2\Im \langle E_{\text{LL}} E_{\text{LL}\perp}^* \rangle \end{bmatrix} \quad (3)$$

In FPS, the polarization basis of the transmit and receive antenna are both synthesized for $-45^\circ \leq \chi_{t,r} \leq 45^\circ$, and $-90^\circ \leq \psi_{t,r} \leq 90^\circ$. Therefore, in FPS, we get the co-pol (receiving antenna polarization is the same as the transmitting antenna) and cross-pol (receiving antenna polarization is orthogonal to that of the transmitting antenna) signature of a target. However, in the compact-pol mode, the transmit antenna polarization is kept constant (i.e., either L or R). We only synthesize the polarization basis of receive antenna ($-45^\circ \leq \chi_r \leq 45^\circ$, and $-90^\circ \leq \psi_r \leq 90^\circ$). Therefore, in CP mode, the received power is given by,

$$\begin{aligned} P_{\text{CP}}(\chi_r, \psi_r) &= \mathbf{g}_r^T \mathbf{K} \mathbf{g}_t \\ &= \mathbf{g}_r^T \mathbf{g}_s \\ &= \begin{bmatrix} 1 \\ \cos 2\chi_r \cos 2\psi_r \\ \cos 2\chi_r \sin 2\psi_r \\ \sin 2\chi_r \end{bmatrix}^T \mathbf{g}_s \end{aligned} \quad (4)$$

where \mathbf{g}_t , \mathbf{g}_s , and \mathbf{g}_r are the Stokes vector describing the polarization state of the transmit antenna, scattered wave, and the receive antenna, respectively. The superscript T denotes vector transpose.

We represent the power computed (P_{FP} and P_{CP}) for all the received and transmitted antenna polarization basis using the 2D contour plots. The FP and CP mode SAR signature will be denoted by FPS and CPS, respectively.

3 Results and Discussion

The FPS and CPS of several canonical and natural targets are analyzed and discussed in the following sections.

3.1 Canonical target analysis

The FPS and CPS (RHV mode) of several canonical targets are shown in Fig. 1 and 2. In the case of a trihedral, the horizontal and vertical co-pol components are equal and in phase. The maximum co-pol power is received for ($\chi = 0^\circ$), i.e., when the polarization of both the transmit and receive antenna is linear. Similarly, the minimum co-pol power is received for ($\chi = 45^\circ$). It informs that for a trihedral target, very low or no power is received when the polarization of both the transmit and receive antenna is circular. One can note from the FPS of trihedral (Fig. 1(a)) that the received power is independent of the ellipse orientation angle (ψ).

The CPS of a trihedral (Fig. 2(a)) exhibits that for a right circular transmit ($\chi = -45^\circ$), the maximum power is received at $\chi = 45^\circ$. It indicates that the scattered wave from a trihedral is polarized orthogonally to the transmitted wave for a circular transmit. The horizontal and vertical co-pol components are equal and out of phase for a dihedral. The FPS of dihedral shows that the maximum co-pol power is received at linear horizontal, linear vertical, and circular polarization (Fig. 1(b)). The minimum co-pol power is received at 45° and 135° linear polarizations. The CPS of a dihedral (Fig. 2(b)) indicates that for a right circular transmit, the maximum power is received at ($\chi = -45^\circ$). Unlike trihedral, for a circular transmit, the scattered wave from a dihedral has the same polarization as the transmitted wave. It is the sole reason for the distinction between a trihedral and a dihedral in CP SAR data.

The FPS of a horizontal (dipole at 0°) and a vertical dipole (dipole at 90°) are shown in Fig. 1(c) and 1(d). They help understand the scattering from vegetation as it is often modeled with a combination of randomly oriented dipoles. The FPS of a horizontal and a vertical dipole looks complimentary to each other. For a horizontal dipole, the co-pol power is maximum for HH ($\chi = 0^\circ$, $\psi = 0^\circ$) polarization and minimum (zero) for VV ($\chi = 90^\circ$, $\psi = 90^\circ$) polarization. Similarly, a vertical dipole has maximum and minimum power at VV and HH polarization, respectively. The canonical nature of the CPS of a horizontal and a vertical dipole is similar to their corresponding FPS (Fig. 2(c) and 2(d)). The respective maximum and minimum received power are similar to FPS.

We usually observe helix scattering from human-made targets that form complex structures. The FPS of the left and right helix is similar, except for their co-pol maximum power, which is found at 45° for the left helix and -45° for right helix (Fig. 1(e) and 1(f)). Such targets can scatter the linearly polarized waves as circularly polarized waves. In CPS, for a right circular transmit, no power is received from

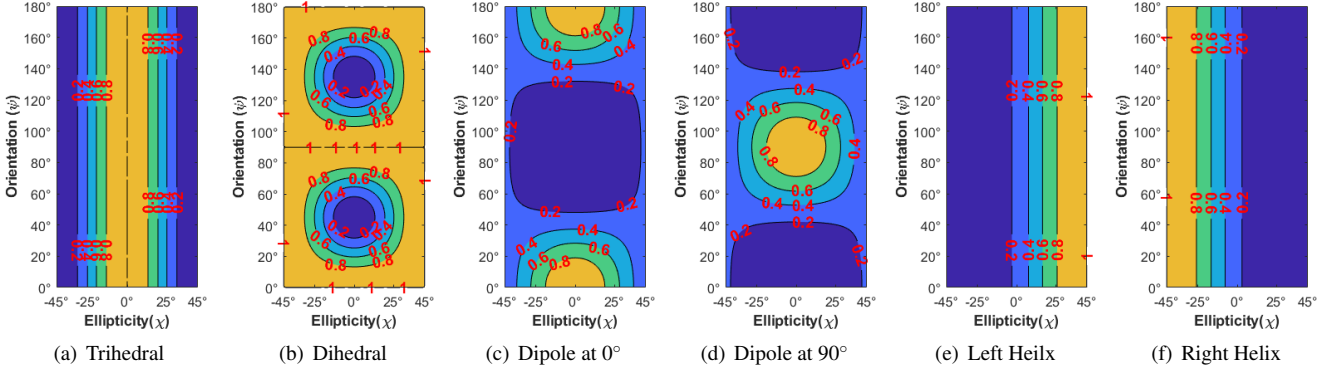


Figure 1. The co-pol full-polarimetric signature (FPS) of (a) Trihedral, (b) Dihedral, (c) Dipole at 0° , (d) Dipole at 90° , (e) Left Helix, and (f) Right Helix. The contour represents the received power.

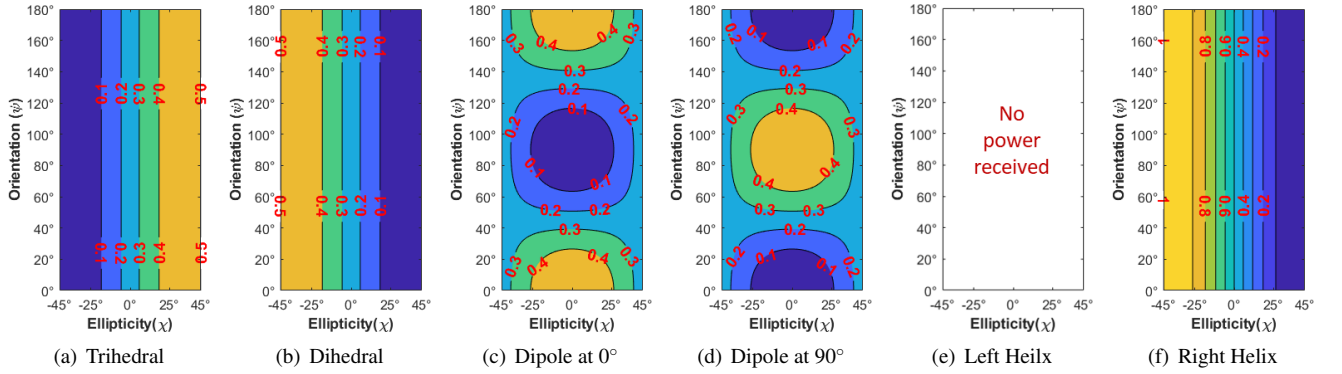


Figure 2. The compact-pol signature (CPS) for RHV polarization mode of (a) Trihedral, (b) Dihedral, (c) Dipole at 0° , (d) Dipole at 90° , (e) Left Helix, and (f) Right Helix. The contour represents the received power.

the left helix (Fig. 2(e)). However, for a right helix, the CPS is similar to the FPS. The maximum power of a right helix is received at -45° .

The FPS of several canonical targets is discussed in detail in [3]. The observed signature from a natural or a human-made target can be related to the canonical target signature to infer the dominant scattering contribution.



Figure 3. Full-polarimetric (FP) C-band Radarsat-2 data over San Francisco Bay area.

3.2 Natural & human-made target analysis

In this section, we analyze the CPS of various natural targets, viz. waterbody (W), orthogonal urban (U), Oriented urban (OU), and vegetation (V) shown in Fig. 3. We show the FPS of different natural and human-made targets in

Fig. 4. The FPS of the W is similar to the signature of a trihedral (FPS). The maximum and minimum co-pol received power was found at $\chi = 0^\circ$ and $\psi = 86^\circ$ (Fig. 4(a)). The maximum power around VV polarization can be related to Bragg scattering from the rough ocean surface. Similarly, the FPS of W is comparable to the signature of a trihedral (CPS). One can observe that for RHV mode, the maximum power of W is received at $\chi = 41^\circ$ (Fig. 5(a)).

The FPS of U is similar to the signature of a dihedral (FPS). The HH and the VV co-pol components are high and almost equal, and high power is received for circular polarization (Fig. 4(b)). In CPS, unlike W, the maximum power is received at $\chi = -34^\circ$ (Fig. 5(b)). One should note that for W, the sense of transmitted wave is changed from right circular to left circular. However, in the case of the U, the sense remains the same as the transmit. Therefore, using the CPS, one can conveniently differentiate between a W (trihedral) and U (dihedral).

We found the FPS of OU to be similar to a rotated dihedral. The maximum power is received at $\chi = -16^\circ$ and $\psi = 144^\circ$ (Fig. 4(c)). Such a signature is unique and can be related to urban targets oriented to the radar line of sight. In CPS, the signature of OU can be confused with the signature of U (Fig. 5(b) and 5(c)). However, the peak power and the variations in the received power differ notably.

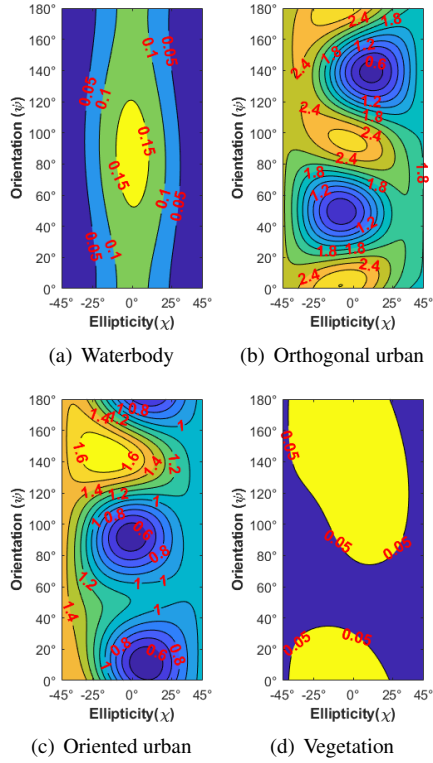


Figure 4. The co-pol full-polarimetric signature (FPS) of (a) Waterbody, (b) Orthogonal urban, (c) Oriented urban, and (d) Vegetation.

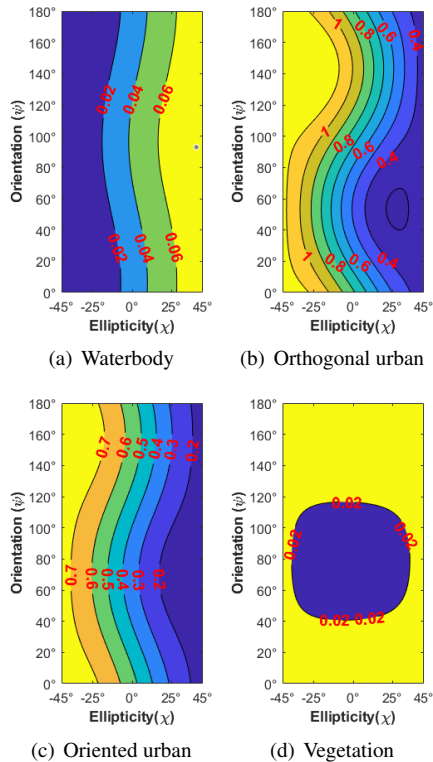


Figure 5. The compact-pol signature (CPS) for RHV polarization mode of (a) Waterbody, (b) Orthogonal urban, (c) Oriented urban, and (d) Vegetation.

The FPS and CPS over V show no significant variation in received power with a change in χ and ψ (Fig. 4(d) and 5(d)). It is possible because the received power is distributed over all the χ and ψ . There exist no particular polarization structure of such targets. It can be characterized with the help of "pedestal height (PH)," which is defined as the ratio of minimum and maximum received co-pol power [3]. We observed a high PH of 0.32 for V.

We observed significant variations in the signatures of different natural and human-made targets. These signatures can be very beneficial in identifying and characterizing natural and human-made targets.

3.3 Conclusion

The study presents a new methodology for analyzing compact-pol (CP) SAR data. We found that the compact-pol signature (CPS) better discriminates several canonical, natural, and human-made targets. The variation in the received power with varying χ and ψ was found beneficial in differentiating waterbody, different types of the urban area, and vegetation. We plan to characterize CPS for various land cover targets in the future. It will also be interesting to assess the variation in CPS at different operating frequencies and incidence angles.

References

- [1] S. R. Cloude and E. Pottier, "A review of target decomposition theorems in radar polarimetry," *IEEE transactions on geoscience and remote sensing*, vol. 34, no. 2, pp. 498–518, 1996.
- [2] F. T. Ulaby and C. Elachi, "Radar polarimetry for geoscience applications," 1990.
- [3] J. J. Van Zyl, H. A. Zebker, and C. Elachi, "Imaging radar polarization signatures: Theory and observation," *Radio science*, vol. 22, no. 04, pp. 529–543, 1987.
- [4] J. Strzelczyk and S. Porzycka-Strzelczyk, "Identification of coherent scatterers in SAR images based on the analysis of polarimetric signatures," *IEEE Geoscience and remote sensing letters*, vol. 11, no. 4, pp. 783–787, 2013.
- [5] A. Verma, D. Haldar, and A. Bhattacharya, "Polarimetric signature analysis of various crop-types using multi-source dual-frequency SAR data," *Geocarto International*, pp. 1–22, 2021.
- [6] A. Verma, S. Dey, N. Bhogapurapu, C. López-Martínez, and A. Bhattacharya, "Dual polarimetric SAR signature for human-made target characterization," in *2021 IEEE International India Geoscience and Remote Sensing Symposium (InGARSS)*. IEEE, 2021, pp. 520–523.